JOURNAL OF MECHANICS OF CONTINUA AND MATHEMATICAL SCIENCES
www.journalimcms.org

ISSN (Online) : 2454 -7190 , Special Issue, No.-10, June (2020) pp 302-330 ISSN (Print) 0973-8975

SUPRASUBDUCTION NATURE OF LATE CRETACEOUS MAGMATISM IN THE MONGOL–OKHOTSK SECTOR OF THE PACIFIC FOLD BELT: GEOCHEMICAL AND SR-ND ISOTOPE EVIDENCES

Inna M. Derbeko

Institute of Geology and Natural Management of Far Eastern Branch of Russian Academy of Sciences, Blagoveshchensk, Russia

Corresponding author: Inna M. Derbeko

E-mail: derbeko@mail.ru

https://doi.org/10.26782/jmcms.spl.10/2020.06.00021

Abstract

The aim of this study is to examine the changes in the petrogenetic model of Late Mesozoic magmatism and the geodynamic evolution of the eastern edge of the Mongol-Okhotsk sector of the Pacific fold belt. The paper presents new Sr-Nd isotope and geochemical data, which were integrated with previously obtained results. It was found that magmatic events experienced three stages: Late Jurassic to 120 Ma; 105–101 Ma; and 95–90 Ma. All rocks are impoverished in Ta, Nb, Sr, Zr. Rocks of the first stage differ from later formations by low concentrations of Rb, Th, U. The isotope characteristics vary within the following values: $(^{87}Sr/^{86}Sr)_t$ = 0.7064–0.7089; $(^{143}Nd/^{144}Nd)_t$ = 0.5123–0.5126.The model age is $T_{(DM-2)}$ ~1.25 Ga. The sequence of magmatic rock formation in the Mongol-Okhotsk sector of the Pacific folded belt is proposed, and sources of igneous melts are identified. It is shown that the Mongol-Okhotsk sector had subduction setting in the Late Mesozoic.

Keywords: Magmatism, subduction, Mesozoic, geochemistry, isotopic data, Mongol–Okhotsk orogenic belt, Pacific folded belt.

I. Introduction

Mesozoic magmatic rocks have long been of interest to researchers due to their obvious link to the high metallogenic potential of the studied region [XX]. This paper presents a reconstruction of magmatic and, respectively, geodynamic stages of development of the eastern edge of the Mongol-Okhotsk orogenic belt and hence the geological evolution of the belt itself in the Late Mesozoic. The author seeks to contribute to the study of development features of the West Pacific Continental Margin.

This work considersmagmatic rocks of Unerikan, Selitkan and Aezop-Yamalin zones of the Mongol-Okhotsk sector of the Pacific folded belt (Fig. 1a).

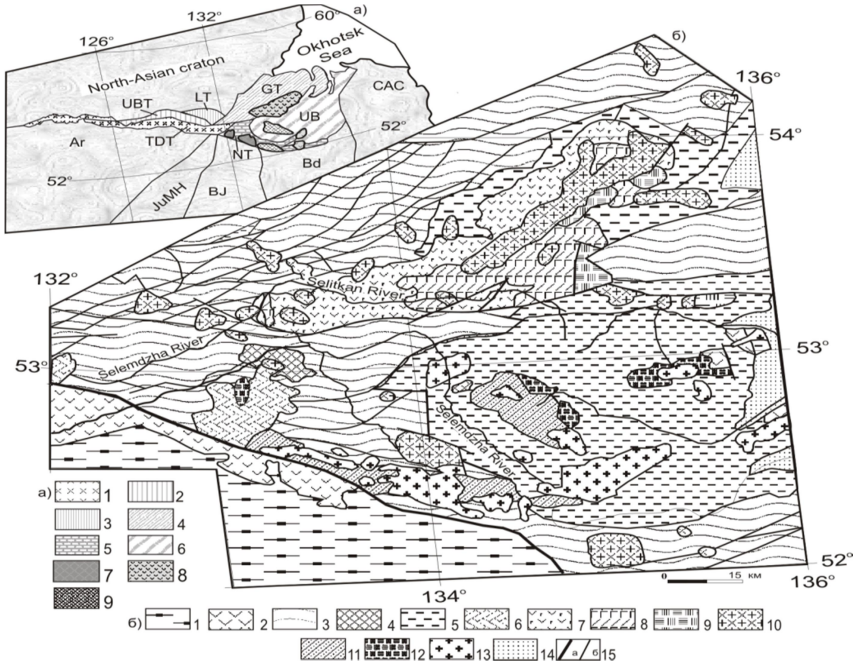

Fig. 1(a): Structural-tectonic scheme of the eastern link of the Mongol-Okhotsk orogenic belt and its framing ([5] with additions). Terrains: 1 – Tukuringra-Dzhagdy, 2 – Unya-Bom, 3 – Lansk, 4 – Galam, 5 – Nilan, 6 – Ulban.
Reference letters: Ar – Argun, SMK – South Mongol-Khingan, BJ – Bureya-Jiamusi, Bd –Badzhal, SAS – Sikhote-Alin – North-Sakhalin.
Volcano-plutonic zones: 7 – Unerikan, 8 – Selitkan, 9 – Aezop-Yamalin.

The original Sr-Nd isotopic and geochemical evidences and the previously obtained data on the geochronology and material composition of magmatic rocks in these zones [XI, XII, XIII;XIV, XV, XVI, VII, XXXIX, XXVIII; XXXII, XXXIV] made it possible to reconstructthe sequence of magmatite formation, to identify the sources of melts from which the magmatites crystallized, and to decode the geodynamic conditions for the formation of volcanoplutonic zones in the Mongol-Okhotsk sector of the Pacific folded belt.

I.i. Tectonic Position and Geological Structure of Volcanoplutonic Zones of the Eastern Edge of the Mongol-Okhotsk Orogenic Belt

By the end of the Late Jurassic the Mongol-Okhotsk sector of the Pacific folded belt was a collage of fragments of Paleozoic and Early Mesozoic accretionary prisms, composed of oceanic sediments (Fig. 1a).

Notably, rocks, formed in deep-sea conditions under the influence of turbidite flows, prevailin the structure of Lansk, Unya-Bom and Ulban terranes. Oceanic basalts and silicon-based minerals occur infrequently. Sediments in the Galam, Tukuringra-Dzhagdy and Nilan terranes are clayshales, aleurolites, sandstones,

silicas, limestones, and in some cases by turbidites [XX]. However, continental volcanoplutonic complexes, which could be categorised as 'stapling' magmatic formations in this region, appeared only in Galam, Ulban and Nilan terranes in the Late Mesozoic. The earliest of those formations are the magmatic rocks of the Unerikan zone [I, XII, X, VII].*Circa* 15 Malater, volcanoplutonic complexes of the Selitkan zone were formed 105 to 101 Ma [II, XIII, X], and after 5 Ma more igneous rocks of the Aezop-Yamalin zone were shaped 95 to 90 Ma [XII, X, XIV, XV].

The Unerikan volcanoplutonic zone is located along the southern boundary of the eastern link of the Mongol-Okhotsk orogenic belt. It is represented by two volcanic areas of 200 and 600 km^2 that stretch to the north-east. The rocks overlap and penetrate the Paleozoic volcanogenic-siliceous and Middle Jurassic terrigenous deposits of the Nilan terrane. In the southwest, the volcanic areas are terminated by a tectonic interface between the Mongol-Okhotsk belt and the Bureya-Jiamusi superterrane (Fig. 1a).

The zone is composed of the rocks of the Unerican complex that includes a sheet (about 600 m thick), vent and subvolcanic facies [II, I]. The lower plane of sheet facies is composed of roughly sorted tuffaceous sedimentary formations, which vertically alternate with interstratified aleuropelitic, psammitic and lithovitroclastic tuffs and felsic lavas. Earlier assumptions [II] were that the upper part of the section included andesite lavas. However, other observations [XXXII] would seem to suggest that these rocks are dated at 102 Ma, which is comparable to the age of lavas of the Selitkanvolcanoplutonic zone (105 to 101 Ma). The affinity of andesites, previously attributed to the Unerikan formations of, and Selitkan andesites can be confirmed not only by their age and structural position of the former in the section, but also by their geochemical characteristics [XIII, XII].

Tuffaceous sandstones from a section on the right bank of the Unerikan River demonstrate a wide range of plant remains [II, I]: *Cyathidites australes* Coup., *C. minor* Coup., *Duplexisporites gyratus* Schug., *Leptolepidites verrucatus* Coup., *Concavisporites junctus* (K.-M.) E. Sem., *Stereisporites compactus* (Bolch.) Jlj., *Klukisporites variegatus* Coup., *Tripartina variabilis* Mal., *Dyctyophyllidites harrisii* Coup., *Neoraistrickia rotundiformis* (K.-M) Taras.The taxonomic composition indicates that the accumulation of volcanic-sedimentary rocks occurred in the Late Jurassic [II]. The K-Ar dating of felsic volcanic rocks, obtained by bulk sampling from the same section, gave closely matching results from 136 to 134 Ma [XXXIX]. According to [XXXIV], outflow of lavas occurred at a later time *c.* 120 Ma, too. Consequently, it can be assumed that the formation of the entire complex began with the accumulation of volcanic-sedimentary component in the Late Jurassic and ended with the outflow of felsic lavas in the Early Cretaceous (*c.* 120 Ma).

The Selitkan Volcanoplutonic Zone is represented by one of the largest volcanoplutonic structures of the West Pacific region. Its geological formations comprise a 200km long eponymous ridge, and the area of the plutonic component considerably extends the distribution area of these rocks. The latter fact suggests that the area of development of volcanoplutonic complexes forming the Selitkan zone

significant expanded within the eastern edge of the Mongol-Okhotsk belt. Most likely, subsequent tectonic events, including the imposition of the Ulban terrane on the Nilan formations, [II, VIII] led to a sharp reduction in the cover facies rocks and brought to the surface of the granitoid masses—the plutonic component of the volcanic-plutonic complexes of this zone.

The volcanic formations that can be singled out in the Selitkan zone overlap,with a sharp inconformity, the terrigenous continental molasse (the Tylskysuite) of the Aptian/Albian times [II, XIII, XII, XXVIII, XXIV] and complex turbidite and volcanogenic-siliceous dislocations of the Nilan and Galam terranes in the eastern edge of the Mongol-Okhotsk orogenic belt (Fig. 1b).

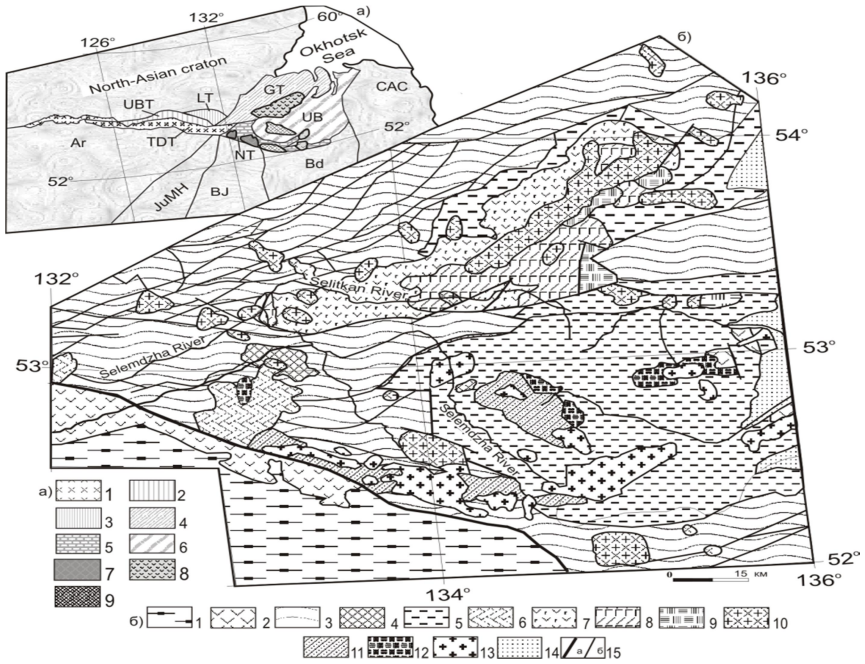

Fig. 1(b): Geological structure of the eastern edge of the Mongol-Okhotsk orogenic belt. Bureya-Jiamusi superterrane (1–2): Paleozoic plutonic formations – 1, Mesozoic volcanogenic-terrigenous formations – 2.
Mongol-Okhotsk orogenic belt (3–5): Paleozoic paleoceanic rocks – 3, Paleozoic plutonic rocks – 4, Mesozoic terrigenous rocks – 5.
Formations of volcanoplutonic zones (6–13): Unerikan felsic volcanites from the Late Jurassic to the Early Cretaceous – 6; Selitkan intermediate to base rocks of the Early Cretaceous – 7, felsic volcanites – 8, subvolcanic bodies – 9, plutonic bodies – 10; Aesop-Yamalin felsic to intermediate volcanites of the Late Cretaceous – 11, subvolcanic bodies – 12, plutonic bodies – 13. Quaternary deposits – 14. Tectonic boundaries (15): interface of the Mongol-Okhotsk folded belt and Bureya-Jiamusi superterrane – 15a, others – 15b. (The figure is based on [II]).

The first fact indicates that it is in the post-Albian age that the accumulation of coarse tuffaceous rocks and lava-breccia begins. Later, after a perturbation, during which the inconformity occurred, both felsic and base lavas and tuffs expanded the section. Magmatites are divided into two volcanoplutonic complexes. The earlier one (Inaragda complex dated 105–102 Ma) has a predominantlyintermediate composition: andesibasalts, andesites, and rarely dacites (Fig. 2a).

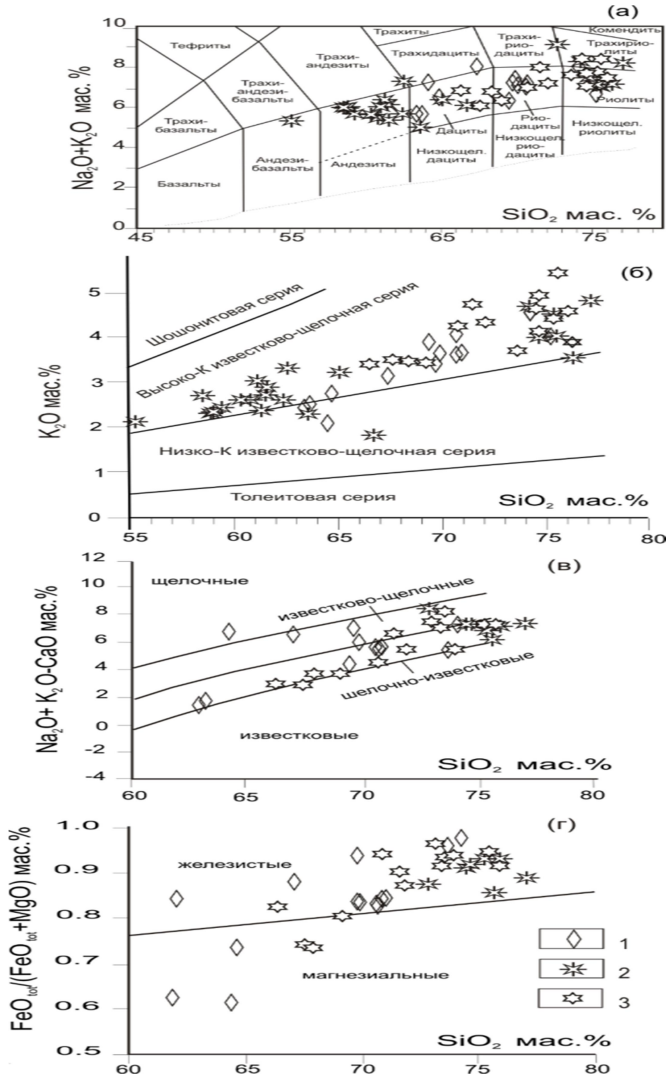

Fig. 2: Petrochemical diagrams for rocks of the volcanic-plutonic zones: Unerikan – 1, Selitkan – 2, Aezop-Yamalin – 3; (a) Na_2O+K_2O - SiO_2 [IV], (b) Na_2O+K_2O - SiO_2 [XXII]; (c) Na_2O+K_2O - SiO_2 [XVII]; (d) Na_2O+K_2O - SiO_2 [XVII].

Its stratified formations make powerful, up to 2200 m, overriding masses. The Inaragda rocks give way to re replaced by the formations of 850 m thick Baranchzha complex, which is represented by rhyolites and trachyrhyolites (Fig. 2a) dated 101 Ma [XVI]. The development of volcanites of the cover facies is accompanied by establishing of subvolcanic, vent and plutonic formations. Subvolcanic bodies are represented by analogues of lavas and diorite porphyrites, quartz diorite porphyrites, granodiorite-porphyries in the first case and granite-porphyries in the second case. All plutonic rocks are united in the Selitkan complex of diorite-granodiorite-granites [II, XXIV]. They compose extended arrays, dikes and small bodies. The central part of the main volcanic structure (the Selitkan Range) is formed by a linear chain of contiguous granite bodies that are up to 85 km long and about 10 km wide [XXXI, XXIV]. According to [II], granodiorites from the subvolcanic bodies can be dated at 105±2 Ma, as determined by the U-Pb technique applied to zircons, or102±1.4 Ma, as determined by the K-Ar technique applied to hornblende and biotites.

The Aezop-Yamalin volcanoplutonic zone is identified within the Nilan and Ulban terranes of the Mongol-Okhotsk orogenic belt. It is represented by two scattered volcanic structures: Aezopand Yam-Alin [XII, XIV, XV], as well as a series of plutonic bodies. More than 120 km long and 30 km wide, the Aezop volcanic structure rests onPaleozoic rocks of the Nilan terrane (Fig. 1b). In the southwest, the zone is confined to the Paukan fault, a tectonic interface between the Mongol-Okhotsk belt and the Bureya-Jiamusi superterrane. The Yam-Alin volcanic structure is just over 50 km long and up to 20 km wide. Its formations unconformably overlaythe early Middle Jurassic terrigenous deposits of the Ulban terrane (Fig. 1b).

The rocks forming the Aezop-Yamalin zone are represented by the cover, subvolcanic and plutonic facies. Two strata are distinguished in the cover facies: the dacite-rhyolite one (lower) and the rhyolite one (upper) [II, XXXI, XIV, XV]. Tuff-terrigenous rocks are scarce, and tuffs predominate over lavas and ignimbrites. The total thickness of stratified formations does not exceed 700 m. Subvolcanic formations play an important role in the zone's structure. Plutonic rocks, which are co-magmatic with volcanites, are combined into the Aezopian intrusive granite-leucogranite complex [XXIV].

Volcanites of the cover facies of the Aezop-Yamalin volcanoplutonic zone are dated90.4±1.4 Ma, as determined by the U-Pb technique applied to zircons [XV]. Taking into account the Rb-Sr and U-Pb dating of granitoids (95.2±0.7 Ma and 94.8±2.2 Ma, respectively [II]), it is assumed that the Aezop-Yamalin volcanoplutonic zone was formed from 95 to 90 Ma [XV].

II. Materials and Methods

This work is based the author's research dataover the past decade. More than 300 samples collected in volcanoplutonic zones of the eastern edge of the Mongol-Okhotsk orogenic belt were analyzed. This paper presents 52 most representative samples (Table 1).

Table 1.2:

Zone	Unerikan			Selitkan							
Sample	d154*	B 29-2	B 47	s1025-9	d15	d8	s1024-5	d8-1	d162*	d18-2	d18-1
Element	12	13	14	15	16	17	18	19	20	21	22
SiO_2	74.01	74.18	75.18	55.04	58.53	58.96	58.98	59.13	59.60	60.34	60.90
TiO_2	0.17	0.02	0.14	0.67	0.61	0.71	0.97	0.65	0.82	0.64	0.64
Al_2O_3	13.32	14.16	13.04	15.39	15.42	16.75	17.97	16.32	16.94	15.91	16.09
$Fe_2O_3^*$	2.27	3.02	1.88	7.48	6.02	5.83	6.13	5.71	7.45	5.76	6.24
MnO	0.03	0.04	0.04	0.14	0.09	0.08	0.10	0.09	0.13	0.10	0.09
MgO	0.21	0.06	0.42	7.16	3.67	3.60	2.64	3.46	3.83	3.65	3.33
CaO	1.17	0.81	0.42	4.96	5.05	5.47	6.29	5.15	5.69	4.65	4.88
Na_2O	2.80	3.48	3.79	3.31	3.20	3.66	3.58	3.31	3.35	3.00	2.91
K_2O	5.35	4.57	3.98	2.07	2.76	2.28	2.38	2.41	2.10	2.67	2.63
P_2O_5	0.04	0.04	0.04	0.12	0.12	0.17	0.25	0.13	0.20	0.13	0.14
Other	0.50	0.53	0.77	3.63	2.31	2.06	0.68	2.68	0.37	2.43	1.66
Total	99.99	99.96	100.01	99.96	97.77	99.00	99.99	99.05	100.5	99.27	99.50
Li	29.1	71	-	64.72	24.82	20.13	11.07	39.56	21.19	8.45	8.95
Rb	268	149	-	66	83	81	73	86	64.91	22	39
Cs	10	7.84	-	2.18	2.12	3.10	6.3	2.34	4.70	0.69	2.70
Sr	113	57	188	252	160	281	277	183	245	49	83
Ba	432	90	-	372	307	421	382	328	360	112	176
La	31.00	13.39	-	12.62	16.76	18.24	16.71	17.18	19.20	4.98	9.63
Ce	68.20	28.14	-	25.11	37.65	40.48	34.02	38.26	45.33	11.09	20.98
Pr	8.41	3.42	-	3.47	4.20	4.65	4.76	4.32	4.94	1.30	2.38
Nd	30.92	13.94	-	14.61	16.68	19.00	19.27	17.37	19.00	5.27	9.26
Sm	6.92	4.02	-	2.7	3.19	3.73	3.94	3.44	4.00	1.03	1.76
Eu	0.46	0.19	-	0.8	0.66	0.89	1.12	0.79	0.95	0.21	0.36
Gd	7.27	3.83	-	3.11	3.79	4.39	3.29	4.03	3.59	1.28	2.08

Tb	1.26	0.6	-	0.51	0.43	0.52	0.67	0.48	0.48	0.14	0.23
Dy	7.61	2.7	-	2.78	2.55	3.13	3.44	2.89	3.45	0.89	1.45
Ho	1.56	0.37	-	0.56	0.48	0.57	0.67	0.53	0.80	0.16	0.26
Er	3.91	0.71	-	1.77	1.46	1.72	1.94	1.64	2.26	0.49	0.80
Tm	0.77	0.09	-	0.28	0.17	0.20	0.28	0.19	0.33	0.05	0.08
Yb	4.49	0.41	-	1.63	1.33	1.47	1.62	1.53	2.36	0.44	0.73
Lu	0.70	0.05	-	0.26	0.17	0.18	0.26	0.20	0.37	0.05	0.07
Y	45	20	19	14.61	13.43	15.62	17.06	14.71	20.40	4.21	7.88
Th	17.9	10.27	-	6.54	8.44	7.53	7.09	8.94	7.10	2.17	4.39
U	4.79	3.78	-	1.72	2.13	1.37	1.8	2.25	2.00	0.60	1.07
Zr	124	52	104	85	123	39	128	136	146	31	65
Hf	3.4	2.29	-	2.47	-	-	3.62	-	4.15	-	-
Nb	9	13	9	4.37	6.12	6.34	6.44	5.92	8	1.71	3.41
Ta	1.4	1.19	-	0.39	-	-	0.55	-	0.71	-	-
Co	3.14	0.82	-	26.45	14.22	16.28	13.92	14.80	16.80	4.25	6.64
Ni	11.38	10.97	-	97.46	31.68	29.08	21.48	36.19	35.81	9.85	14.16
Sc	6.47	4.55	-	20.62	13.28	15.16	12.69	13.69	13.50	3.91	6.65
V	9.85	2.6	-	144.8	89.72	112.38	111.14	98.71	85.40	26.60	46.39
Cr	71.06	54.31	-	314.9	118.21	125.52	81.19	105.00	120.50	35.52	52.37
Ti	916	56	839	4016	3657	4250	5815	3897	3759	3975	3837
ASI	0.83	1.16	1.15	0.93	0.89	0.93	0.91	0.95	0.96	0.98	0.99

Table 1.3:

Zone	Selitkan										
Sample	d10	d2	s1026-14	s3177-4	d5	s1028-3	d11	a3207-1	d4	d13-0	d14
Element	23	24	25	26	27	28	29	30	31	32	33
SiO_2	60.99	61.29	61.58	61.58	62.34	62.44	63.54	65.00	66.70	72.80	74.15
TiO_2	0.63	0.65	0.68	0.66	0.63	1.06	0.60	0.56	0.39	0.13	0.11
Al_2O_3	15.96	16.91	15.92	16.25	15.67	16.02	15.82	14.82	16.8	13.83	13.1

									2		4
$Fe_2O_3^*$	5.46	5.33	5.56	5.67	5.33	6.38	4.84	4.90	3.10	1.64	2.67
MnO	0.09	0.09	0.09	0.08	0.08	0.09	0.09	0.06	0.07	0.05	0.04
MgO	3.39	2.65	3.69	3.44	3.61	1.09	3.19	3.31	1.22	0.24	0.27
CaO	4.62	3.95	4.63	5.44	4.87	3.37	3.24	4.10	3.15	0.79	0.85
Na_2O	2.98	3.99	3.25	2.65	3.00	4.07	2.74	2.91	4.16	3.82	3.53
K_2O	3.01	2.37	2.89	2.72	2.62	3.34	2.21	3.42	1.79	5.31	4.67
P_2O_5	0.14	0.13	0.14	0.12	0.13	0.21	0.13	0.11	0.14	0.04	0.03
Other	1.83	2.21	1.68	1.33	1.42	2.03	3.05	0.76	1.81	0.49	0.30
Total	99.09	99.59	100.12	99.98	99.69	100.09	99.45	100.03	99.36	99.14	99.75
Li	25.62	38.53	15.89	13.99	27.26	13.09	18.72	31.5	24.99	23.81	23.80
Rb	102	67	86	99	92	130	79	134	45	1744	128
Cs	2.74	0.65	1.68	10.38	5.48	2.68	3	8.85	1.84	8.27	4.12
Sr	212	225	186	199	203	197	176	192	398	59	51
Ba	408	396	376	376	407	479	590	3940	394	482	458
La	21.00	17.25	17.08	18.44	20.38	20.33	19.10	22.91	14.35	35.11	27.52
Ce	46.23	38.06	36.85	41.88	45.92	44.23	42.96	52.34	30.73	72.24	57.76
Pr	5.33	4.30	4.75	4.81	5.06	6.02	4.85	5.73	3.39	7.62	6.05
Nd	21.32	17.43	19.95	19.82	19.97	25.1	18.89	21.45	13.43	26.72	21.12
Sm	4.05	3.46	3.99	4.02	3.91	5.78	3.53	4.36	2.50	4.39	3.46
Eu	0.82	0.81	0.9	0.83	0.77	1.12	0.72	0.74	0.60	0.44	0.35
Gd	4.64	4.18	3.5	3.41	4.64	4.57	4.02	4.04	2.88	5.27	3.92
Tb	0.56	0.50	0.51	0.6	0.55	0.79	0.45	0.7	0.30	0.59	0.42
Dy	3.25	3.07	2.97	3.69	3.27	4.51	2.73	3.76	1.79	3.54	2.52
Ho	0.60	0.58	0.6	0.7	0.61	0.88	0.48	0.72	0.29	0.67	0.45
Er	1.81	1.75	2.23	2.2	1.85	3.03	1.46	1.99	0.89	2.21	1.48
Tm	0.22	0.21	0.3	0.31	0.22	0.38	0.16	0.31	0.08	0.29	0.18
Yb	1.67	1.60	1.57	1.73	1.69	2.32	1.33	1.86	0.76	2.33	1.47
Lu	0.22	0.20	0.25	0.26	0.21	0.33	0.01	0.28	0.07	0.33	0.20
Y	16.38	15.53	15.66	17.5	16.43	22.6	13.07	21.4	8.70	19.06	12.91

Th	11.32	7.64	11.6	10.71	10.85	10.83	10.02	14.23	3.78	28.15	20.59
U	2.71	2.07	2.76	3.27	2.83	2.95	2.00	3.2	0.69	6.18	4.29
Zr	131	111.61	158.19	136.57	141.98	194.92	130.84	192	20.27	105.69	82
Hf	5	-	5	4.28	-	6.56	-	1.64	-	-	-
Nb	7.17	5.93	6.5	6.3	7.45	8.49	7.37	8.9	5.02	10.90	8.53
Ta	-	-	0.63	0.66	-	0.73	-	0.91	-	-	-
Co	14.60	13.61	14.13	14.94	15.22	13.25	12	15.45	4.70	1.29	1.62
Ni	40.44	15.37	35.18	25.29	47.28	4.86	24.1	37.39	3.81	2.48	10.62
Sc	13.26	12.71	12.21	14.87	14.06	14.84	11	11.59	4.74	2.76	2.37
V	92.54	87.23	83.5	86.45	95.25	126.96	63.872	81.8	32.66	3.10	5.87
Cr	131.22	70.22	102.91	99.39	182.67	44.52	93.682	132.14	89.69	105.52	78.06
Ti	3759	3758	3447	3553	4322	5773	6355	3333	3333	2338	1067
ASI	0.97	1.04	0.94	0.96	0.95	0.98	1.20	0.93	1.10	1.03	1.07

Table 1.4:

Zone	Selitkan					Aezop-Yamalin					
Samples	d16-3	s1001-2	d13-2	d16	s3179-6	d1430	d125	d10504	d5153-2*	d157	d107-3
Elements	34	35	36	37	38	39	40	41	42	43	44
SiO_2	74.78	75.19	75.28	76.13	77.06	66.30	67.58	68.24	69.01	70.66	71.52
TiO_2	0.11	0.04	0.13	0.10	0.13	0.40	0.39	0.38	0.34	0.23	0.26
Al_2O_3	13.55	13.79	12.66	12.77	12.07	16.29	14.69	15.01	14.24	15.46	14.23
Fe_2O_3	1.88	1.34	1.53	1.89	1.36	4.02	6.11	3.51	3.55	3.09	3.37
MnO	0.05	0.03	0.04	0.02	0.02	0.10	0.04	0.05	0.07	0.04	0.03
MgO	0.17	0.1	0.25	0.15	0.16	0.83	0.51	1.26	0.85	0.17	0.36
CaO	0.16	0.38	1.04	0.14	0.39	3.98	2.86	3.23	2.75	2.54	1.50
Na_2O	3.54	2.63	3.04	3.71	3.39	3.44	2.43	3.35	2.94	2.83	3.15

K_2O	3.93	4.54	4.02	3.51	4.81	3.48	3.63	3.51	3.44	4.19	4.87
P_2O_5	0.03	0.02	0.02	0.03	0.02	0.09	0.09	0.09	0.07	0.05	0.07
Other	1.36	1.67	1.04	1.17	0.64	0.98	1.48	0.40	1.44	0.47	0.43
Total	99.54	99.74	99.05	99.63	100.05	100.07	99.96	99.05	98.72	99.97	99.99
Li	13.23	19.93	25.63	16.48	12.65	28.2	22.1	-		24.3	32.4
Rb	101	130	138	86	196	107	107	113	153	104	185
Cs	1.92	3.02	6.82	1.14	2.12	6	76	-		5	9
Sr	27	50	90	25	53	241	197	195	173	303	329
Ba	483	565	507	380	471	600	635	526	1198	1395	881
La	25.79	11.17	27.05	23.33	29.18	31.86	28.10	-	-	38.61	30.64
Ce	54.75	29.01	56.88	48.94	65.14	66.74	59.54	-	-	82.27	69.19
Pr	5.74	3.68	5.97	5.15	7.19	7.73	6.78	-	-	9.33	7.75
Nd	19.61	13.67	20.71	17.72	24.06	27.71	26.37	-	-	33.29	29.31
Sm	3.22	3.60	3.33	2.86	4.61	5.89	5.56	-	-	6.49	5.74
Eu	0.30	0.56	0.35	0.28	0.48	0.93	0.90	-	-	1.04	0.93
Gd	3.62	2.55	3.98	3.20	3.22	4.98	5.38	-	-	5.58	5.45
Tb	0.37	0.38	0.42	0.32	0.51	0.82	0.98	-	-	0.89	0.88
Dy	2.17	1.60	2.52	1.82	2.62	4.66	5.75	-	-	5.30	4.74
Ho	0.40	0.34	0.47	0.32	0.6	0.89	1.03	-	-	0.97	0.92
Er	1.35	0.80	1.55	1.12	1.41	2.78	3.23	-	-	2.74	2.56
Tm	0.16	0.14	0.19	0.13	0.25	0.41	0.61	-	-	0.48	0.43
Yb	1.41	0.85	1.59	1.17	1.31	2.56	3.66	-	-	2.65	2.27
Lu	0.18	0.10	0.21	0.15	0.22	0.41	0.50	-	-	0.40	0.36
Y	11.59	8.27	13.59	9.95	16.50	28	32	-	-	30	28
Th	20.14	8.02	22.48	18.93	20.50	10.69	10.17	-	-	10.5	13.9
U	4.42	1.70	5.19	4.32	2.54	2.36	2.24		-	2.21	3.04
Zr	80	54	81	74	80	169	152	-	-	175	128
Hf	-	2.25	-	-	3.14	2.9	2.4	-	-	3.2	3.0
Nb	5.90	7.87	8.530	7.20	8.67	8	8	-	-	7	11

Ta	-	0.58	-	-	0.79	0.8	0.7	-	-	0.7	1.1
Co	0.82	1.01	0.81	0.78	1.28	7.36	10.79	-	-	176.31	5.3
Ni	1.43	2.55	1.11	3.69	4.31	11.2	14.71		-	8.32	12.67
Sc	1.88	2.60	1.87	1.65	1.65	12.16	9.82	-	-	8.32	7.52
V	2.73	4.88	6.89	2.86	2.14	32.69	40.00	-	-	11.28	15.97
Cr	46.37	52.60	70.52	50.28	35.60	60.66	68.02	-	-	87.72	47.85
Ti	509	240	239	767	721	2220	1985	-	-	1320	1317
ASI	1.32	1.30	1.10	1.20	1.05	1.25	1.27	1.40	1.18	1.13	0.90

Table 1.5:

Zone	**Aezop-Yamalin**							
Sample	d 2153-1	da3051*	d 158	d156*	j10603	e3021-1	d 21-34	br-1548
Elements	45	46	47	48	49	50	51	52
SiO_2	71.95	73,79	74.44	74.56	74.56	75.18	75.52	75.78
TiO_2	0.31	0,076	0.16	0.19	0.16	0.09	0.06	0.06
Al_2O_3	13.92	14,27	13.70	12.82	13.40	12.66	12.55	13.04
Fe_2O_3*	3.31	2,15	1.80	2.87	2.19	2.39	0.82	1.29
MnO	0.05	0,095	0.05	0.04	0.02	0.03	0.01	0.04
MgO	0.48	0,155	0.16	0.29	0.14	<0.05	0.06	0.12
CaO	1.82	0,41	0.31	1.08	1.79	0.73	0.50	0.13
Na_2O	2.98	3,89	3.30	2.98	3.07	3.35	2.70	2.92
K_2O	4.29	3,76	4.99	4.62	4.12	4.45	5.70	4.60
P_2O_5	0.07	0,05	0.04	0.05	0.03	0.02	0.02	0.03
Other	0.65	0,86	0.95	0.43	0.38	0.26	0.63	1.39
Total	99.99	99,96	100.01	100.00	100.01	99.94	98.57	99.43
Li	52.9		39.8	25.1	25.6	25.7	-	-
Rb	143	102	151	162	92	159	146	164
Cs	4	2.43	7	7	2	3	-	-
Sr	163	131	86	71	155	85	267	70

Ba	774	575	515	259	792	717	364	240
La	29.82	15,22	43.17	32.39	60.31	29.57	-	-
Ce	63.67	31,82	94.73	69.14	125.18	67.15	-	-
Pr	7.37	3,56	10.29	8.09	14.23	7.94	-	-
Nd	25.71	12,94	39.31	29.99	48.99	30.02	-	-
Sm	5.35	2,63	8.58	6.21	7.91	6.85	-	-
Eu	0.71	0,52	0.58	0.36	0.80	0.52	-	-
Gd	5.07	2,13	9.34	5.98	5.75	6.67	-	-
Tb	0.82	0,32	1.74	1.04	0.78	1.16	-	-
Dy	4.57	1,29	9.43	5.88	3.69	6.88	-	-
Ho	0.96	0,2	1.98	1.27	0.64	1.35	-	-
Er	2.77	0,51	5.71	3.36	1.87	3.84	-	-
Tm	0.46	0,06	0.80	0.53	0.30	0.70	-	-
Yb	2.58	0,4	4.46	3.17	1.76	3.60	-	-
Lu	0.44	0,06	0.70	0.47	0.24	0.56	-	-
Y	28	6.45	57	34	20	40	-	-
Th	13.06	6.65	16.9	15.8	13.80	13.6	-	-
U	2.70	1.38	2.56	5.29	1.25	2.70	-	-
Zr	152	130	112	71	136	104	-	-
Hf	2.7	2.13	2.8	3.2	2.3	4.3	-	-
Nb	11	7	9	10	7	11	-	-
Ta	0.9	0.59	0.9	1.1	0.5	0.9	-	-
Co	4.73	1.35	2.25	2.28	4.96	2.02		-
Ni	8.68	5.31	5.43	6.55	1.77	14.07		
Sc	7.71	1.48	5.91	4.36	-	7.86	-	-
V	15.33	0.02	8.19	5.57	-	3.6	-	-
Cr	51.35	112.97	21.34	79.18	-	59.31	-	-
Ti	1718	455	640	895	950	443	-	-
ASI	0.97	0.99	0.84	0.97	0.79	0.85	0.74	0.88

The content of petrogenic elements (main petrogenic components Sr, Zr, Nb) in the samples was determined by X-ray fluorescence (XFR) analysis using the S4 PIONEER spectrometer in the Institute of Geology and Nature Management, Far East Branch of the Russian Academy of Sciences (Blagoveshchensk, Russia). Analysis of the rare-earth elements (Ga, Ge, Rb, Cs, Sr, Ba, Pb, La, Ce, Pr, Nd, Sm, Eu, Gd, Tb,

Dy, Ho, Er, Tm, Yb, Lu, Y , Th, U, Zr, Hf, Nb, Ta, Sc) was made inductively coupled mass spectrometry (ICP-MS)in the Institute of Analytical Instrumentation of the Russian Academy of Sciences (Saint Petersburg, Russia).

To perform the XFR analysis, the powder sample was homogenized by fusion with lithium metaborate (flux) in a muffle furnace at 1,150 °C. The measurements were carried out using Pioneer 4S X-ray spectrometer (Bruker, Germany). The intensity values of analytical lines were adjusted against the background, absorption and secondary fluorescence. For the ICP-MS analysis, the samples were extracted by acid decomposition. The measurements were carried out on the PlasmaQuad spectrometer (VG Elemental) in standard mode. The sensitivity calibration over the entire mass scale was performed using a multi-element standard solution of rare-earth elements (produced by Matthew Johnson). The relative error of measurements was 3–10% [XI, XII, XIV].

Rhyolites from the Selitkan zone were dated by the U-Pb technique applied to zircons in the Institute of Geology and Geochronology of the Precambrian of the Russian Academy of Sciences (St. Petersburg, Russia) [XVI].

For geochronological $^{40}Ar/^{39}Ar$ study of Aezop-Yamalin lavas, a matrix was isolated from a sample of trachyrhyolite that completes the formation of volcanic extrusive sheets [XV].

The Rb, Sr, Sm and Nd contents and $^{87}Rb/^{86}Sr$ and $^{147}Sm/^{144}Nd$ isotope ratios for 8 rock samples were determined in the Institute of Geology of Ore Geology, Petrography, Mineralogy, and Geochemistry of the Russian Academy of Sciences under the guidance of A.V. Chugaev [VII]. The isotope dilution method with mixed ^{85}Rb–^{84}Sr and ^{149}Sm–^{150}Nd tracers was used in these studies. The tracers were added to the samples immediately before their chemical decomposition. The decomposition of gross rock samples, which weighed from 0.1 to 0.2 g, was carried out in concentrated acid mixture HF + HNO_3 (3:1). The samples were kept in a hermetically sealed autoclave at 160 °C until complete dissolution.

The Rb, Sr, Sm and Nd specimen for mass spectrometric analysis were obtained using two-step ion-exchange chromatography. First, Rb and Sr fractions and light REE fractions were separated from the elements of the sample matrix. Separation was carried out in 2.4 M HCl in ion exchange columns filled with 3 ml of cation exchanger BioRad W50x8 (200-400 mesh). Second, Nd and Sm were chromatographically separated from other light REE, using columns filled with 0.5 ml of ion exchange resin HDEHP applied to Kel-F pellets. The total level of background contamination of the sample during the chemical preparation procedure for Sr and Nd did not exceed 0.1 ng.

Mass spectrometric measurements of Rb, Sr, Sm and Nd isotopic composition were carried out using multi-collector thermal ionization mass spectrometer Sector 54 (Micromass, the UK). The measurement accuracyfor $^{87}Sr/^{86}Sr$ and $^{143}Nd/^{144}Nd$ isotope ratios was verified by systematic comparison to the isotopic reference SRM 987 and the intralaboratory isotopic reference Nd-IGEM calibrated against the La Jolla

international standard. The error in the measured $^{87}Sr/^{86}Sr$ and $^{143}Nd/^{144}Nd$ ratios did not exceed 0.003% ($\pm 2\sigma_{unit}$). The accuracy of $^{87}Rb/^{86}Sr$ and $^{147}Sm/^{144}Nd$ isotope ratios was 0.5% and 0.2%, respectively ($\pm 2\sigma_{unit}$).

III. Results

III.i. Petrochemical and Geochemical Analysis

Volcanic rocks of the Unerikan zone are represented by felsic lavas: trachyrhyolites, rhyolites, rhyodacites, dacites, and trachidacites. They can be high-potassium and, if SiO_2 content is less than 65%, low-potassium representatives of the calc-alkali series (Fig. 2a,b,c); mainly ferruginous or, if SiO_2 content is less than 65%, magnesian (Fig. 2d); the alumina saturation index (ASI) varied from 0.8 to 1.1 (Table 1), in an individual case to 1.6. The REE distribution spectra of the Unerikan formations (Fig. 3a) showed that LREE clearly dominates over HREE ((La/Yb)n = 11.42–13.57) with a weakly pronounced Eu anomaly ((Eu/Eu*)n = 0.52–0.70). Vulcanites can be characterized by relatively lower concentration of Nb (7.47–9.25 g/t), Ta (0.64–1.19 g/t), Sr (52–220 g/t), Zr (52–178 g/t), Ti (50–3,000 g/t), Y (12–18 g/t), and Yb (0.41–1.83 g/t). Refer to Fig. 3b and Table 1.

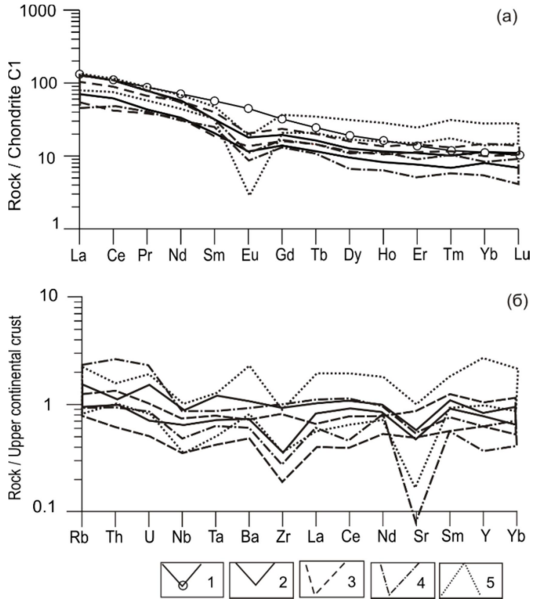

Fig. 3: REE concentrations in the Late Mesozoic rocks of the Mongolo-Okhotsk sector, normalized to the compositions of chondrites (a) and continental crust (b). OIB composition (1). Composition of the rocks by zone: Unerikan (2); Selitkan intermediate to base (3), Selitkan felsic (4); Aezop-Yamalin (5). Recalculation: a) according to [XXXV]; b) according to [XXX].

Nearly all magmatites of the Selitkan zone belonged to the high-potassium calc-alkali series (Fig. 2b), having increased calcareousness of felsic formations (Fig. 2c). The ASI values in the intermediate to base rocks were found to be 0.89–0.99, in individual cases up to 1.20 (Table 1). In felsic formations the ASI values increased from 0.93 to 1.32, and the concentration of iron was also higher (Fig. 2d).

In volcanites from the andesite rocks the REE distribution was moderately fractionated $(La/Sm)_n$ = 2.2–2.9; $(La/Yb)_n$ = 5.3–7.4, while in plutonic comagmatic rock these values were slightly higher $(La/Sm)_n$ = 3.3; $(La/Yb)_n$ = 8.4. The fractionation of lanthanides in felsic rocks was more pronounced $(La/Sm)_n$ = 1.9–3.9; $(La/Yb)_n$= 8.9–15.1.Here, we found a stable negative europium anomaly (Eu/Eu*) = 0.36–0.53, while this ratio in andesitoids approaches one (Eu/Eu*) = 0.53–0.92 (Fig. 3a). The relative de-enrichment withhigh field strength elements Nb, Ta, Hf, Zr, Sr and the enrichment with LREE and large-ion lithophilic elementsBa, Rb, K, Li, Th, U was established in all types of formations (Table 1) [XIII]. Such behaviour of the elements (except for Sr) is rather peculiar to magmatic rocks of continental volcanic arcs [XXVI]. The Th/U ratio approaches four, which characterizes the rocks as formations of active continental margins [III]. The ratio La/Ta >20 [XXIX] suggests the same conditions.

Lava-pyroclastic flows of the Aezop-Yamalin zone included dacites, rhyodacites, trachyrhyodacites, rhyolites, trachyrhyolites. Plutonic formations, which are co-magmatic with lavas, were represented by granite-porphyries, subalkaline granite porphyries, subalkaline leucogranite-porphyries and leucogranite-porphyries (Figure 2a). These are high-potassium, predominantly alkaline-calcareous, ferruginous (magnesian in certain cases) rocks with ASI = 0.81–1.2 (Fig. 2b,c,d;Table 1).

The lanthanide distribution spectra showed a slight predominance of LREE over HREE and a pronounced negative Eu anomaly, which was highlighted by $(La/Yb)_n$ = 4.5–9.2 and Eu/Eu* = 0.1–0.5 (Fig. 3a). The geochemical features of magmatites in the studied zone included a moderate enrichment with Ba, Rb, Ce, Th, and REE while such elements as Nb, Ta, Sr were depleted (Table 1, Fig. 3b).

By the nature of element distribution, the rocks are comparable to volcanites of marginal continental belts. This is also evidenced by the ratios La/Yb = 6–14 (predominantly less than 10), La/Ta> 22, Th/U = 3.3–4.8.

III.ii. Rb-Sr and Sm-Nd Isotope Studies

The Rb-Sr and Sm-Nd isotope characteristics were determined for two samples of Unerikan rocks [VII]: rhyodacite and trachyrhyolite (Table 2). The calculated ratios $^{87}Sr/^{86}Sr$ and $^{143}Nd/^{144}Nd$ in them at the time of formation (120 Ma) were found very close. The ratios $(^{87}Sr/^{86}Sr)_t$ and $(^{143}Nd/^{144}Nd)_t$ in rhyodacite were 0.7074 and 0.512379 (or in relative units $\varepsilon_{Nd(T)}$ = -3.8); in trachyrhyolite, 0.7066 and 0.512411,respectively ($\varepsilon_{Nd(T)}$= -3.5).

Table 2: Results of Rb-Sr and Sm-Nd studies of magmatic rocks of the Mongol-Okhotsk sector of the Pacific fold belt

Sample	Complex	Age (Ma)	Rock	Rb (µg/g)	Sr (µg/g)	$^{87}Rb/^{86}Sr$ ±2σ	$^{87}Sr/^{86}Sr$ ±2σ	Sm (µg/g)	Nd (µg/g)	$^{147}Sm/^{144}Nd$ ±2σ	$^{143}Nd/^{144}Nd$ ±2σ	$^{87}Sr/^{86}Sr_{(t)}$	$\varepsilon_{Nd(T)}$
B-28	Unerikan	120	rhyodacite	140	196	2.07 ±1	0.710937±12	4.9	25	0.1165±2	0.512379±10	0.7074	-3.8
D 154	Unerikan	120	trachyriolite	202	93	6.28 ±2	0.717266±10	7.4	32	0.1380±1	0.512411±10	0.7066	-3.5
D 155	Aezop-Yamalin	90	granite-porphyry	99	268	1.072 ±3	0.709045±10	4.8	24	0.1186±9	0.512361±10	0.7076	-4.5
D 157	Aezop-Yamalin	90	granite-porphyry	112	275	1.179 ±4	0.709524±10	4.3	23	0.1146±3	0.512348±10	0.7079	-4.7
D 156	Aezop-Yamalin	90	rhyolite	96	138	1.998 ±7	0.710484±11	7.6	50	0.0919±1	0.512354±10	0.7078	-4.3
D 162	Selitkan	105	andesite	84	315	0.769 ±3	0.708116±10	4.3	21	0.1229±2	0.512488±10	0.7070	-1.9
D-162-1	Selitkan	105	andesibasalt	42.9	461	0.2695±14	0.709268±10	2.7	12.9	0.1275±3	0.512546±10	0.7089	-0.9
D-162-3	Selitkan	105	andesibasalt	20.3	456	0.1291±5	0.706606±10	3.7	16.4	0.1355±3	0.512624±10	0.7064	+0.5

Note to Table 2: The Sr-Nd isotope-geochemical characteristics of rocks ware studied in the the Institute of Geology and Nature Management, Far East Branch of the Russian Academy of Sciences, using traditional methods of chemical sample preparation and mass spectrometric analysis [V]. The background level for the chemical preparation of samples was Sr < 0.15 ng and Nd < 0.1 ng. Analysis of the Rb, Sr, Sm, Nd isotopic composition was performed on multi-collector thermal ionization mass spectrometer Sector 54 (Micromass, the UK).

The measurement accuracy for $^{87}Sr/^{86}Sr$ and $^{143}Nd/^{144}Nd$ isotope ratios was verified by systematic comparison to the isotopic reference SRM 987 and the intralaboratory isotopic reference Nd-IGEM calibrated against the La Jolla international standard.

The error in the measured $^{87}Sr/^{86}Sr$ and $^{143}Nd/^{144}Nd$ ratios did not exceed 0.003%. The accuracy of $^{87}Rb/^{86}Sr$ and $^{147}Sm/^{144}Nd$ isotope ratios was 1% and 0.2%, respectively ($2\sigma_{unit}$).

The Rb-Sr and Sm-Nd isotopic data were obtained for three samples of andesite and andesite basalts from the Selitkan zone (Table 2). The values $(^{87}Sr/^{86}Sr)_t$ were found to be 0.7064–0.7089, which is close to the values established for igneous rocks of the Aeszop-Yamalin and Unerikan complexes. The $\varepsilon_{Nd(T)}$ valuewas much higher (from -1.9 to +0.5).

The Rb-Sr and Sm-Nd isotope characteristics (Table 2) were also obtained for two samples of granite-porphyry and one sample of rhyolite [VII]. Magmatites of theUnerikan and Selitkan zones typically showed very consistent initial Sr-Nd values, higher $(^{87}Sr/^{86}Sr)_t$ ratios (from 0.7076 to 0.7079) and the lowest$\varepsilon_{Nd(T)}$values (from -4.3 to -4.7).

IV. Discussions

The evolution of the Mongol-Okhotsk sector of the Pacific folded belt in the Late Mesozoic has been the subject of discussions to date. According to some researchers [XXI], in the Mesozoic this region developed under the conditions of a transform continental margin. Other authors believe that the territory was an active continental margin, within which the forming magmatic complexes accompanied subduction processes and (or) a shift from subduction setting in the Early Cretaceous to collision setting in the Late Cretaceous [XXVII]. However, it is commonly agreed that it was the tectonic rearrangements of the region in the Late Mesozoic that led to the appearance of a series of volcanoplutonic zones [XXXI, XX].

All the considered volcanoplutonic zones have felsic varieties of igneous rocks. If compared to the composition of the upper continental crust (Fig. 3b), their composition points to an evident depletion of Ta, Nb, Sr, Zr. At that, felsic rocks of the Selitkan and Aezop-Yamalinzones demonstrate changes in the content of certain elements: the concentration of Ce, La, Nd, Ba, Y, Yb, Sr increases from the earlier rhyolites (101 Ma) of the Baranchzha complex in the Selitkan zone to younger rhyolites (95–90 Ma) of the Aezop-Yamalin zone (Fig. 3b). There is evidence that such changes in heterochronous igneous rocks occur with the development of volcanic arcs [XXVI]. The Unerikan rhyolites do not correspond to this sequence: in addition to the above elements, they were found to have lower Rb, Th, U concentrations, as compared tofelsic volcanites of the other two zones (Fig. 3b).

The relative proximity of the initial $^{87}Sr/^{86}Sr$ and $^{143}Nd/^{144}Nd$ isotopic ratios in the rocks of these zones suggests that they crystallized from magmas from reservoirs with similar Sr-Nd isotope characteristics (Table 2). The $(^{87}Sr/^{86}Sr)_t$и $(^{143}Nd/^{144}Nd)_t$ values suggest that there should be a significant portion of the Neoproterozoic continental crust matter in magmas, from which the Unerikan and Aezop-Yamalin rocks crystallized (Fig. 5).

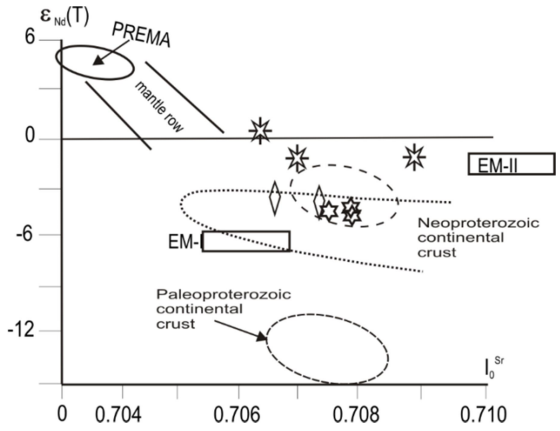

Fig. 5: Late Mesozoic igneous rocks of volcanic-plutonic zones of the eastern edge of the Mongol-Okhotsk belt in the diagram $\varepsilon_{Nd}(T)$ - $^{87}Sr/^{86}Sr$. The dotted lines show the hypothesized fields of Sr and Nd isotope composition for the continental crust in the Neoproterozoic and Late Archean-Paleoproterozoic ages; dots show the field of the continental crust of the Central Asian fold belt according to [XVIII]. The fields PREMA, EMI, EMII are shown according to [XXXVII, XXXVIII] The Sr and Nd isotope composition for the DM type mantle sources are calculated for 100 Ma. Also, see caption to Fig. 4.

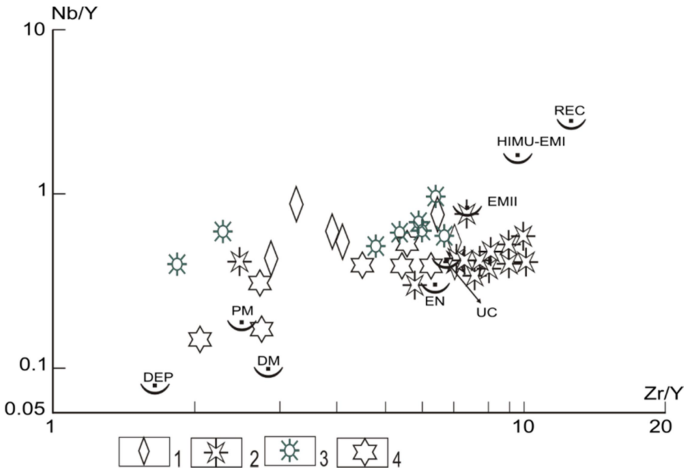

Fig. 4: Compositions of Late Mesozoic magmatic rocks of volcanic-plutonic zones of the eastern edge of the Mongol-Okhotsk belt in the Nb/Y - Zr/Y diagram and their relation to typical magmatic sources. Magmatic sources are given according to [VI]: DEP – deep depleted mantle, DM – shallow depleted mantle, PM – primitive mantle, EN – enriched component, EMII – enriched mantle with high Nd/Sm, HIMU-EMI – enriched mantle with high (?) U/Pb, UC – upper continental crust, REC – recycled component. Rocks by zones (1–4): Unerican – 1, Selitkan intermediate to base – 2,

Selitkan felsic – 3; Aezop-Yamalin – 4.

This assumption can be confirmed by the model age of the rocks: $T_{(DM-2)}$ ~1.25 Ga (mean value estimated by the rocks of the Unerikan and Aezop-Yamalin complexes: b28, d155, d157; refer toTable 2). Similar data are given in [XXXIII], where the Neoproterozoic model age $T_{(DM-2)}$ ~ 1.3 Ga, is also indicated for rhyodacites of the Unerikan zone. As shown in Fig. 5, the values of felsic formations of these zones fall into the assumed field of the Sr and Nd isotope composition for the continental crust of the Neoproterozoic age and in the field of the continental crust of the Central Asian fold belt, according to [XVIII]. At the moment it is known that Precambrian formations are present at the section bases of the Galam and Tukuringra-Dzhagdy terranes [XX].

In the former case they are represented by ultramafites, while Late Proterozoic limestones with oncolites and cathographies are present at the base of the присутствуют terrane. Based on the comparability of the material composition and the age of the rocks of the Nilan and Tukuringra-Dzhagdy terranes, it was suggested that these are disjoint fragments of a single accretion complex [XX]. Therefore, it can be assumed that such rocks may occur in the Nilan terrane. Unfortunately, there are no data on the isotope composition of felsic rocks of the Selitkan zone, and the values for Selitkan intermediate to base volcanites are shifted towards the PREMA field (Fig. 5). The spread of ratios $(^{143}Nd/^{144}Nd)_t$ in andesites of the Selitkan zone (Table 2) may indicate the possible participation of magmas of various origins in their formation.

In the Nb/Y–Zr/Y ratio diagram (Fig. 4), the compositions of all felsic magmatic formations of the region are located in the fields corresponding to the enriched component (EN) and the upper continental crust (UC). Formations of the Unerikan zone have a different location in the Nb/Y–Zr/Y diagram (Fig. 4), which indirectly confirms the assumption that this geological object developed independently.

V. Conclusions

Although insignificant, the differences, found in the initial Sr-Nd characteristics of the rocks of the Unerikan, Selitkan and Aezop-Yamalin zones, probably arise from the initial Sr-Nd isotopic heterogeneity of terranes (blocks) of the continental crust that have undergone melting in the Cretaceous. Such a conclusion can be made by analyzing the geotectonic positions of volcanoplutonic complexes of these zones. Thus, the Unerikan rocks are established exclusively within the structures of the Nilan terrane of the eastern margin of the Mongol-Okhotsk orogenic belt. The Selitkan formations can be found mainly within the Galam terrane; single plutonic bodies noted within the Nilan terrane. The Aezop-Yamalin zone covers the territory of the Nilan and Ulban terranes (Fig. 1).

The crystallization of felsic rocks from magmas, formed during melting of the continental crust, can also be confirmed by high values of the La/Nb ratios (1.4±4.1) [XIX] and low values of the Ce/Y ratios (2.8–3.6). All these data, as well as the distribution of microelements in the volcanoplutonic formations of the studied zones (Fig. 3)—in particular, LREE contents, low Ta and Nb contents, high La/Yb ratios (more than 10) and La/Ta ratios (more than 20)—indicate that magmogenesis involved a substance similar to the substrates of the original magmas of island arcs. This can support the assumption that these magmatic complexes were formed in the geodynamic environment where the active continental margin interacted with the rising mantle diapirs, arising from the melting subducting oceanic plate. As a result, the mixed substances came from different sources: a moderately depleted mantle of a PREMA type, the enriched suprasubduction lithospheric EM mantle, and the continental crust (Fig. 4, Fig. 5).

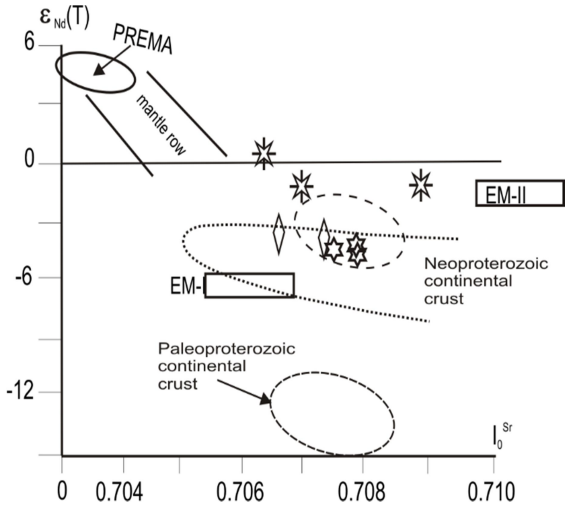

Fig. 5: Late Mesozoic igneous rocks of volcanic-plutonic zones of the eastern edge of the Mongol-Okhotsk belt in the diagram εNd (T) - 87Sr/86Sr. The dotted lines show the hypothesized fields of Sr and Nd isotope composition for the continental crust in the Neoproterozoic and Late Archean-Paleoproterozoic ages; dots show the field of the continental crust of the Central Asian fold belt according to [XVIII]. The fields PREMA, EMI, EMII are shown according to [XXXVII, XXXVIII]. The Sr and Nd isotope composition for the DM type mantle source are calculated for 100 Ma. Also, see caption to Fig. 4.

What speaks in favour of such tectonic scenario is the location of the figurative points of the Mesozoic magmatic formations of the eastern edge of the Mongol-Okhotsk sector on tectonic discriminatory diagrams (Figures 6a, c). The points, indicating the compositions of felsic volcanites and granitoids of the studied zones, are located in the areas of subduction setting, just as the points of the intermediate to base rocks of the Selitkan zone.

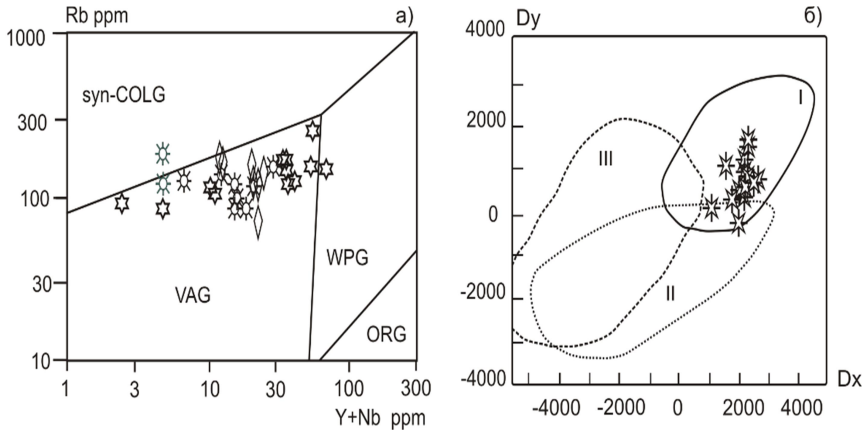

Fig. 6: Discriminatory diagrams, describing the tectonic settings of rock formation: (a) felsic according to [XXVIII]; (b) intermediate to base according to [XXXVI]. Reference letters for felsic rocks: syn-COLG – syn-collision, VAG – island-arc, WPG – intraplate, ORG – orogenic. Fields of intermediate to base rocks concentration: I – island arcs; II – trap; III – continental rifts. Also, see caption to Fig. 4.

Therefore, the obtained geochemical and Sr-Nd isotope characteristics indicate that Late Mesozoic volcanoplutonic complexes of the Mongol-Okhotsk sector of the Pacific folded belt were formed as a result of subduction processes. They are associated with the interaction of the continental margins of Asia and the Isanagi plate, which actively moved northwest in the late Mesozoic, according to paleomagnetic data [XXV]. Following the stages of magmatic activity on the eastern edge of the Mongol-Okhotsk orogenic belt, it can be stated that the movement of the oceanic plate had a pulsating character and corresponded to the time when volcanoplutonic complexes were formed.

The results make it possible to propose a tectonic scheme of the Late Mesozoic subduction setting within the Mongol-Okhotsk sector of the Pacific folded belt (Fig. 7).

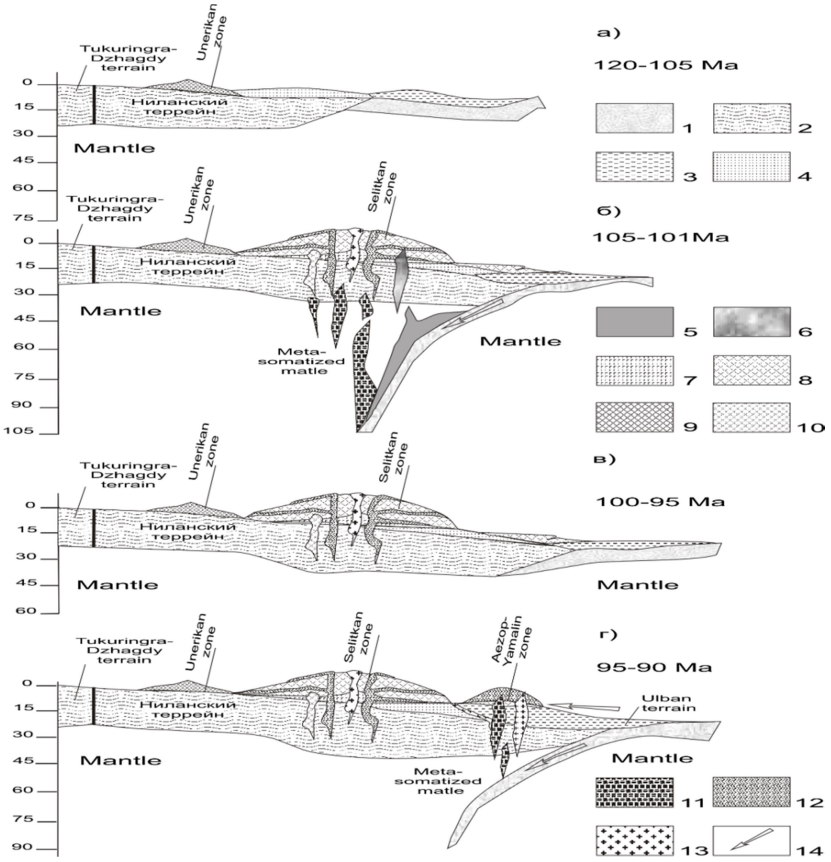

Fig. 7: Model and sequence of formation of the volcanoplutonic zones of the Mongol-Okhotsk sector: 1– oceanic crust; 2 – continental crust; 3 – turbidite sediments; 4 – continental molasse; 5 – adakite melts generated during melting of the subducted oceanic crust; 6 – adakite melts modified when passing the mantle wedge; 7 – andesite basalts, basalts; 8 – rhyolites, rhyodacites, dacites; 9 – andesites; 10 – quartz diorites, granodiorites; 11 – fluids depleted in water but enriched in silica; 12 – rhyolites, trachyrhyolites; 13 – granites, subalkaline granites: 14 – direction of motion of the oceanic plate.

The rocks of the earliest Unerikan complex were distributed only within the Nilan terrane (Fig. 7a). Probabaly, the Nilan terrane was a continental margin in the Late Jurassic and the beginning of the Early Cretaceous. This cannot decidedly determine the time of its inclusion into the Mongol-Okhotsk belt. He could drift on the oceanic plate and join the mainland after the magmatic events in the Late Jurassic and the beginning of the Early Cretaceous. The period from 120 to 105 Ma was marked by the accumulation of continental sediments, when the Nilan terrane was a passive continental margin (Fig. 7a). According to paleomagnetic data [XXXIII], *c*. 119–110 Ma the oceanic was moving north and, naturally, had little influence on the

continent. However, theIzanagi plate turned by almost 30° and accelerated its movement in the north-west direction. During this period (110–85 Ma [XXXIII]) the rocks of the Selitkan volcanoplutonic zone were formed [XIII] (Fig. 7b). The total thickness of the cover facies of this zone was found to be more than 3000 m, taking into account the volume of the plutonic component of the complexes. This undoubtedly led to a significant increase in the thickness of the continental crust in this region and, accordingly, the subduction of the continental margin.

It can be assumed that it is during this period that the Ulban terrane advanced to the formations of the Nilan terrane [II, VIII]. It also led to the enlargement and thickening of the continental crust and the further 'healing' of the thrust zone by the formations of the Aezop-Yamalin complex (Fig. 7d).

All these facts indicate that in the Late Mesozoic the oceanic plate subducted the continental margin in the Mongol-Okhotsk sector of the Pacific folded belt. The subduction settinggradually faded from the Early Cretaceous to the late Cretaceous. At that, in the period from the Late Jurassic to the Early Cretaceous (120 Ma), volcanic activity manifested itself only on the Nilean terrane. The terranecould have adjoined the Asian continent later than the described events, which indicates the independent evolution of this geological object. In the period from 105 to 90 Ma, the subduction was accompanied by the establishment of the Selitkan and Aezop-Yamalin zones. The beginning of these processes can be determined by the formation of intermediate to base rocks of the Selitkan zone. Theircomposition is rather similar to the composition of the rocks in suprasubduction settings. They were replaced byfelsic magmatites of the Selitkan zone (101 Ma) and, later, of the Aezop-Yamalin zone (95–90 Ma). The changes in the material composition of these two zones allow make an assumption about a change in the geodynamic processes, namely, the attenuation of the subduction along the eastern edge of the Mongol-Okhotsk sector of the Pacific folded belt.

VI. Acknowledgements

This research was supported by Russian Foundation for Basic Research, grant 13-05-12043-ofi-m.

References

I. Agafonenko S.G. Asmolova Ye.I. Osobennosti vnutrennego stroyeniya vulkanogennykh tolshch verkhnego techeniya reki Selemdzha [Peculiarities of the internal structure of volcanogenic formation in the upper reaches of the Selemdzha River]. In: Korrelyatsiya mezozoyskikh kontinentalnykh obrazovaniy Dalnego Vostoka i Vostochnogo Zabaykalya [Correlation of Mesozoic continental formations of the Far East and Eastern Transbaikal]. Chita: Chitageolsyomka, 2000. P. 58–59. (in Russian)

II. Agafonenko S.G. State Geological Map of the Russian Federation 1: 200 000, 2nd edition. Tugur Series. Sheet N-53-XXVI.Saint Petersburg: Karpinsky Russian Geological Research Institute, 2002.

III. Allerge G.J., Dupre B., Lewin E. Thorium/Uranium radio of the earth. Chem. Geol. 1986. V. 56. № 3/4. P. 219–227.

IV. Bogatikov O.A. (ed.) Magmaticheskiye gornyye porody [Magmatic rocks], vol.1. Moscow: Nauka, 1983. 367 p. (in Russian)

V. Chernyshev I.V., Bakharev A.G., Bortnikov N.S., Goltsman YU.V., Kotov A.B., Gamyanin G.N., Chugayev A.V., Salnikova Ye.B., Bairova E.D. Geokhronologiya magmaticheskikh porod rayona zolotorudnogo mestorozhdeniya Nezhdaninskoye (Yakutiya, Rossiya): U-Pb, Rb-Sr i Sm-Nd-izotopnyye dannyye [Geochronology of igneous rocks of Nezhdaninskoye gold deposit (Yakutia, Russia): U-Pb, Rb-Sr and Sm-Nd isotope data]. Geologiya Rudnykh Mestorozhdeniy. 2012. V.54. Iss.6. P.487–512. (in Russian)

VI. Condie K.S. Higt field strength .element ratios in Archean basalts: a window to evolving sources of mantle plumes? Lithos. 2005. V.79. P. 491–504.

VII. Derbeko I.M, Chugayev A.V., Oleynikova T.I., Bortnikov N.S. Geokhimicheskiye i Sr-Nd izotopnyye svidetelstva nadsubduktsionnogo proiskhozhdeniya mezozoyskogo magmatizma Mongolo-Okhotskogo sektora Tikhookeanskogo skladchatogo poyasa [Geochemical and Sr-Nd isotopic evidence of the suprasubduction origin of the Mesozoic magmatism of the Mongol-Okhotsk sector of the Pacific folded belt]. Doklady Akademii Nauk. 2016. V. 466. Iss. 4. P. 462–466. (in Russian)

VIII. Derbeko I.M. Polozheniye Ulbanskoy strukturno-formatsionnoy zony v skheme strukturno-formatsionnogo rayonirovaniya [Position of the Ulban structural–formational zone in the scheme of structural–formational zonation]. In: Geologiya i mineralnyye resursy Amurskoy oblasti [Geology and mineral resources of Amur Oblast]. Blagoveshchensk: Amurgeolkom. 1995. P. 70. (in Russian)

IX. Derbeko I.M. Pozdnemezozoyskiy etap evolyutsii vostochnogo zvena Mongolo-Okhotskogo orogennogo poyasa [Late Mesozoic stage of evolution of the eastern link of the Mongol-Okhotsk orogenic belt]. Proceedings of XLVI Tectonic meeting. 2014. V.1. P. 111–115. (in Russian)

X. Derbeko I.M. Pozdnemezozoyskiy vulkanizm Mongolo-Okhotskogo poyasa (vostochnoye okonchaniye i yuzhnoye obramleniye vostochnogo zvena poyasa). [Mesozoic volcanism of the Mongol-Okhotsk belt (the eastern edge and the southern framing of the eastern part]. Saarbryukken: LAMBERT Academic Publishing GmbH&Co.KG. 2012. 97 p. (in Russian)

XI. Derbeko I.M. Pozdnemezozoyskiy vulkanizm Priamur'ya (veshchestvennyy sostav, geokhronologiya, geodinamicheskiye obstanovki) [Late Mesozoic volcanism of the Amur River region (material composition, geochronology, geodynamic conditions)]. PhD Dissertation. Blagoveshchensk: Institute of Geology and Nature Management of the Far East Branch of the Russian Academy of Sciences, 2007. 159 p. (in Russian)

XII. Derbeko I.M. Skhema formirovaniya magmaticheskikh kompleksov Selitkanskoy vulkano-plutonicheskoy zony vostochnogo flanga Mongolo-Okhotskogo orogennogo poyasa (Rossiya) po geokhimicheskim dannym [The Selitkan volcano-plutonic zone, the eastern flank of the Mongol-Okhotsk orogenic belt (Russia): Evidence from geochemical data]. Geokhimiya. 2009. V.11. P. 1155–1172. (in Russian)

XIII. Derbeko I.M., Agafonenko S.G., Kozyrev S.K., Vyunov. D.L. Umlekano-Ogodzhinskiy vulkanogennyy poyas (problemy vydeleniya) [The Umlekan-Ogodzha volcanic belt (the problem of separation)]. Litosfera. 2010. V.3. P. 70–77. (in Russian)

XIV. Derbeko I.M., Sorokin A.A., Agafonenko S.G. Geokhimicheskiye osobennosti kislogo magmatizma severo-zapadnogo flanga Khingano-Okhotskogo vulkano-plutonicheskogo poyasa (Ezopskaya i Yam-Alinskaya zony) [Geochemical features of acid magmatism of the northwestern flank of the Khingan-Okhotsk volcano-plutonic belt (Aezop and Yam-Alin zones)]. Tikhookeanskaya Geologiya. 2008. V.1. P. 61-71. (in Russian)

XV. Derbeko I.M., Sorokin A.A., Ponomarchuk V.A., Travin A.V., Sorokin A.P. Pervyye geokhronologicheskiye dannyye dlya lav kislogo sostava Ezop-Yam-Alinskaya vulkano-plutonicheskaya zona Khingano-Okhotskogo vulkanogennogo poyasa [The first geochronological data for acid lavas of the Aezop-Yam-Alin volcano-plutonic zone of the Khingan-Okhotsk volcanic belt]. Doklady Akademii Nauk. 2008. V.419. Iss.1. P.95–99. (in Russian)

XVI. Derbeko I.M., Sorokin A.A., Salnikova Ye.B., Kotov A.B, Sorokin A.P., Yakovleva S.Z., Fedoseyenko A.M., Plotkina Yu.V. Vozrast kislogo vulkanizma Selitkanskoy zony Khingano-Okhotskogo vulkano-plutonicheskogo poyasa (Dalniy Vostok Rossii) [Age of persilicic volcanism in the Selitkan zone of the Khingan-Okhotsk volcano-plutonic belt (the Far East of Russia)]. Doklady Akademii Nauk. 2008. V.418. Iss.2. P.221–225. (in Russian)

XVII. Frost B.R., Barnes C.G., Collins W.J., Arculus R.J., Ellis D.J., Frost C.D. A geochemical classification for granitic rocks J. Petrology. 2001. V. 42. P. 2033–2048.

XVIII. Guo F., Fan W., Gao X., Li Ch., Miao L., Zhao L., Li H. Sr-Nd-Pb isotope mapping of Mesozoic igneous rocks in NE China: Constraints on tectonic framework and Phanerozoic crustal growth. Lithos. 120. 2010. Pp. 563–578.

XIX. Hoffman A.W. Mantle geochemistry: the message from oceanic volcanism. Nature. 1997. V. 385. P. 219–229.

XX. Khanchuk A.I. (ed.) Geodinamika, magmatizm i metallogeniya Vostoka Rossii [Geodynamics, magmatism and metallogeny of Eastern Russia]. Vladivostok: Dalnauka. 2006. 979 p. (in Russian)

XXI. Khanchuk A.I., Ivanov V.V. Mezo-kaynozoyskiye geodinamicheskiye obstanovki i zolotoye orudeneniye Dal'nego Vostoka [Meso-Cenozoic geodynamic conditions and gold mineralization of the Far East]. Geologiya i Geofizika. 1999. V.40. Iss.11. P.1635–1645. (in Russian)

XXII. Le Bas M., Le Maitre R.W., Streckeisen A., Zanettin B. A chemical classification of volcanic rocks based on the total-silica diagram. J. Petrology. 1986. V. 27. P. 745–750.

XXIII. Lebedev Ye.L. Stratigrafiya nizhnemelovykh otlozheniy Toromskogo progiba (Zapadnoye Priokhot'ye) [Stratigraphy of the Lower Cretaceous deposits of the Torom trough (West Near-Okhotsk Sea district]. Sovetskaya. Geologiya. 1969. V. 8. P. 27–36. (in Russian)

XXIV. Martynyuk M.V., Ryamov S.A., Kondratyeva V.A. Obyasnitel'naya zapiska k skheme raschleneniya i korrelyatsii magmaticheskikh kompleksov Khabarovskogo kraya i Amurskoy oblasti [Explanatory note to the scheme of dismemberment and correlation of magmatic complexes of Khabarovsk Krai and Amur Oblast]. Khabarovsk: TSTP PGO Dalgeologiya, 1990. 215 p. (in Russian)

XXV. Maruyama, S., Seno,T. Orogeny and relative plate motions: example of the Japanese Islands. Tectonophysics. 127. 1986. P. 305–329.

XXVI. Murphy J.B. Igneous Rock Associations 8. Arc Magmatism II: Geochemical and Isotopic Characteristics Geoscience Canada. 2007. V. 34. № 1. P. 7–35.

XXVII. Natalyin B.A., For M. Geodinamika vostochnoy okrainy Azii v mezozoye [Geodynamics of the eastern margin of Asia in the Mesozoic]. Tikhookeanskaya Geologiya. 1991. V.6. P.3–20. (in Russian)

XXVIII. Pearce J. A., Harris N. B., Tindle A.G. Trace element discrimination diagrams for the tectonic interpretation of granitic rocks. J. Petrol. 1984. V. 25. P. 956–983.

XXIX. Puzankov Yu.M., Volynets O.N., Seliverstov V.A. et al. Geokhimicheskaya tipizatsiya magmaticheskikh i metamorficheskikh porod Kamchatki [Geochemical typification of magmatic and metamorphic rocks of Kamchatka]. Novosibirsk: Institute of Geology and Geophysics of Siberian Branch of the USSR Academy of Sciences, 1990. 259 p. (in Russian)

XXX. Rudnick R.L., Gao S. The Composition of the Continental Crust. Oxford: Elsevier/Pergamon, 2003. V. 3. P. 1–64.

XXXI. Shcheglov A.D. (ed.) Vulkanicheskiye poyasa vostoka Azii. Geologiya i metallogeniya [Volcanic belts of East Asia. Geology and metallogeny]. Moscow: Nauka, 1984. 503 p. (in Russian)

XXXII. Sorokin A.A., Kotov A.B., Kovach V.P., Ponomarchuk V.A., Savatenkov V.M. Istochniki pozdnemezooyskikh magmaticheskikh assotsiatsiy Severo-Vostochnoy chasti Amurskogo mikrokontinenta [Sources of Late Mesozoic magmatic associations of the North-Eastern part of the Amur microcontinent]. Petrologiya. 2014. V.22. Iss.1. P.72–84. (in Russian)

XXXIII. Sorokin A.A., Sorokin A.P., Ponomarchuk V.A., Travin A.V. Vozrast i geokhimicheskiye osobennosti vulkanicheskikh porod vostochnogo flanga Umlekano-Ogodzhinskogo vulkanoplutonicheskogo poyasa (Priamurye) [The age and geochemistry of volcanic rocks on the eastern flank of the Umlekan–Ogodzha volcanoplutonic belt (Amur region)]. Geologiya i Geofizika. 2010. V.51. Iss.4. P.473–485. (in Russian)

XXXIV. Sorokin A.A., Sorokin A.P., Salnikova Ye.B., Derbeko I.M., Kotov A.B., Yakovleva S.Z. Geokhronologiya riolitov unerikanskogo kompleksa vostochnogo flanga Umlekano-Ogodzhinskogo poyasa (Dalniy Vostok) [Geochronology of rhyolites of the Unerikan complex of the eastern flank of the Umlekan-Ogodzha belt (Russian Far East). Proceedings of the III Russian Conference on Isotope Geochronology. June 6-8, 2006. Moscow. V.2. P.311–314. (in Russian)

XXXV. Sun S.S., McDonough W.F. In: Magmatism in the oceanic basins (Saunders A.D. & Norry M.J. Eds). Geol. Soc. Spec. Publ. № 42. 1989. P. 313–345.

XXXVI. Velikoslavinsy S.D., Glebovitskiy V.A. Novaya diskriminantnaya diagramma dlya klassifikatsii ostrovoduzhnykh i kontinentalnykh bazaltov na osnove petrokhimichskikh dannykh [A new discriminant diagram for the classification of island-arc and continental basalts based on petrochemical data]. Doklady Akademii Nauk. 2005. V. 401. Iss. 2. P. 213–216. (in Russian)

XXXVII. Weaver B.L. 1991. The origin of ocean island basalt end-member compositions: trace element and isotopic constraints Earth Planet. Sci. Lett. 1991. V. 104. Iss. 2-4. P. 381–397.

XXXVIII. Zindler A., Haris S. Chemical geodynamics. Ann. Rev. Earth Planet. Sci. 1986. V.14. P. 493–571.

XXXIX. Zubkov V.F. State Geological Map of the USSR 1: 200 000. Sheet N-53-XXVI. Moscow: MinGeo, 1975. 116 p.